Gold-Nanocrystal-Enhanced Bioluminescent Nanocapsules

Juanjuan Du,[†,⊥] Jing Jin,[†,‡,⊥] Yang Liu,[†] Jie Li,[†] Talar Tokatlian,[†] Zuhong Lu,[‡] Tatiana Segura,[†] Xu-bo Yuan,[*,§] Xianjin Yang,[§] and Yunfeng Lu[*,†]

[†]Department of Chemical and Biomolecular Engineering, University of California at Los Angeles, Los Angeles, California 90095, United States, [‡]School of Biological Science and Medical Engineering, Southeast University, Nanjing 210096, China, and [§]School of Materials Science and Engineering, Tianjin University, 92 Weijin Road, Nankai District, Tianjin 300072, China. [⊥]These authors contributed equally to this work.

ABSTRACT Metal-enhanced bioluminescence presents a great opportunity to achieve ultrasensitive analysis and imaging with low bioluminescent background and enhanced luminescence. We hereby report metal-enhanced bioluminescence based on bioluminescent protein nanocapsules conjugated with gold nanocrystals. Such gold-nanocapsule complexes exhibit near 10-fold enhancement in bioluminescent intensity and are effectively delivered into the cells with outstanding stability. This work offers a class of bioluminescent nanoparticles for imaging and other applications.

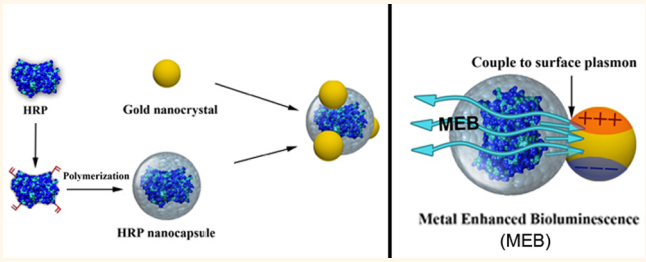

KEYWORDS: metal-enhanced bioluminescence · bioluminescent protein naocapsules · gold nanocrystal · intracellular delivery

Bioluminescence is the light emission resulting from enzymatic reactions within living organisms. Owing to its ultrasensitive detectability, it has been emerging as a platform for various applications,[1−3] including whole-cell biosensors, immunoassays, nucleic-acid hybridization assays, and *in vivo* imaging. Despite the high sensitivity, bioluminescent glows are normally dim, limiting the application in time-sensitive detection.[4,5] By coupling surface plasmon with excitation-state molecules via nonradiative energy transfer, nanocrystals of noble metal are demonstrated to enhance optical phenomena, such as fluorescence,[6−8] chemiluminescence,[9,10] and phosphorescence.[11] However, metal-enhanced bioluminescence is insufficiently investigated. Conjugating noble metal nanocrystals to bioluminescent proteins only resulted in bioluminescence quenching.[12] It still remains challenging to create a metal-enhanced bioluminescence agent toward time-sensitive bioluminescence detection.

We hypothesize that nanocrystals of a noble metal can amplify bioluminescence, similar to other metal-enhanced optical phenomena, leading to enhanced luminescence intensity and reduced decay time. In this research, we present a bioluminescent protein nanocapsule (BPN) design consisting of a bioluminescent protein (light-emission module) and gold nanocrystals (light-enhancement module). Particularly, horseradish peroxidase (HRP) is used as a model bioluminescent system. HRP catalyzes the oxidation of luminol to 3-aminophthalate, accompanied by light emission at 425 nm (Scheme 1A). Instead of native HRP, we used HRP nanocapsules[13−16] to load the gold nanocrystal on the luminol. Protein naonocapsules contain a single protein inside a polymer layer formed by *in situ* polymerization.[13,17,18] Scheme 1B illustrates the synthetic route of the nanocapsules. First, we conjugated a polymerizable vinyl group to HRP by reacting its lysine groups with *N*-acryloxysuccinimide (step I). Subsequent *in situ* polymerization with acrylamide (neutral) and *N*-(3-aminopropyl)methacrylamide (cationic) as the monomers resulted in HRP nanocapsules (denoted as nHRP) containing surface amine groups (step II). Gold nanocrystals capped with 3-mercaptopropionic were then conjugated to nHRP (step III), yielding bioluminescent-protein nanocapsules (BPNs). With this BPN structure, the energy generated by the bioluminescence reaction can be effectively coupled with gold nanocrystals, emitting enhanced luminescence with reduced decay time (Scheme 1C).

* Address correspondenc to xbyuan@tju.edu.cn, luucla@ucla.edu.

Received for review March 20, 2014 and accepted September 22, 2014.

Published online September 22, 2014
10.1021/nn504371h

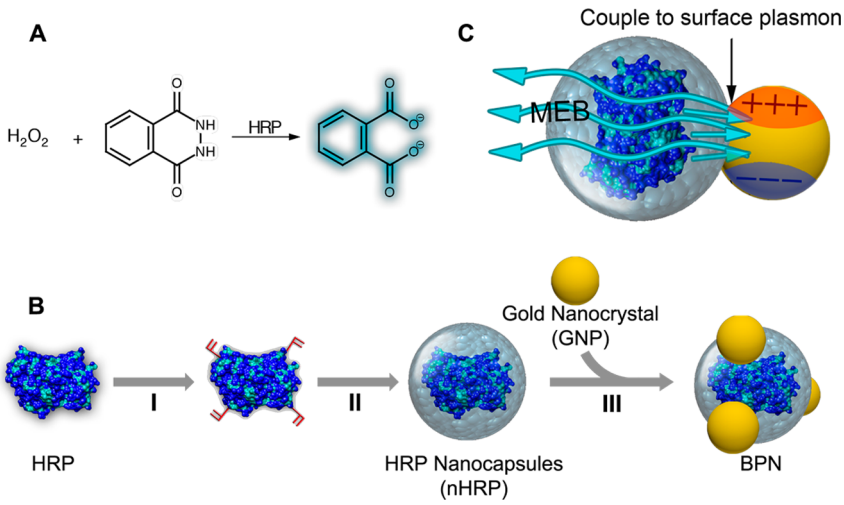

Scheme 1. Schematic illustration of (A) the luminescence reaction catalyzed by HRP; (B) strategy of synthesizing gold-nanocrystal conjugated HRP nanocapsules (BPNs); and (C) bioluminescence enhancement of BPNs achieved through the coupling effect.

This unique architecture offers several major advantages: (1) The nanocapsule structure stabilizes the interior protein, addressing the stability issues associated with direct use of bioluminescent proteins. (2) Encapsulating bioluminescent protein within the nanocapsules addresses another major issue associated with direct use of bioluminescent proteins, poor cell permeability, enabling their use as intracellular reporting system (such as firefly luciferase) (Scheme 1C). (3) The polymer layer serves as a spacer to provide suitable distance between protein and metal particles for optical enhancement. (4) Such nanocrystal–bioluminescent conjugates possess nanoscale size (~tens of nanometers), enabling versatile uses for various applications. Note that we have recently conjugated semiconductor quantum dots (e.g., CdTe) onto bioluminescent nanocapsules. Utilizing the resonance energy transfer process between the quantum dots and subsequent bioluminescent emission, bioluminescent nanocapsules with tunable emission wavelength (e.g., from 425 to 754 nm) were produced.[15] However, such conjugation systems could offer neither any signal enhancement nor decay time reduction.

RESULTS AND DISCUSSION

Preparation of Gold-Nanocrystal-Conjugated HRP Nanocapsules. Figure 1 panels A and B respectively show transmission electron microscopic (TEM) images of gold nanocrystals (GNC) and nHRP. As-synthesized gold nanocrystals exhibit uniform diameters around 8 nm; while nHRPs show an average diameter of 27 nm, which is confirmed by dynamic light scattering (DSL) measurements (Supporting Information, Figure S1). Considering the diameter of native HRP is around 3 nm,[19] the average shell thickness of each nHRP is estimated within the range of 10 nm. The structure of BPN is also clearly revealed under TEM observation (Figure 1C), demonstrating the conjugation of gold nanocrystals to nHRP. Figure 1D shows the agarose gel electrophoresis pattern of GNC and BPNs. Because of their surface ligands (3-mercaptopropionic acid), GNCs exhibit negative charge, migrating toward the anode. After conjugation with cationic nHRP, the GNC–nHRP complexes (BPNs) exhibit net positive charge (zeta potential, 7.33 mv; Supporting Information, Figure S2) and migrate toward the cathode in the agarose gel. The formation of BPNs is also confirmed by visible absorption spectrum. GNC has a characteristic absorption at 525 nm, to which their surface plasmon resonance contributes. After conjugation to nHRP, a red shift (~7 nm) in the GNC surface plasmon absorption (Figure 1E) was observed, suggesting that conjugating nHRP with GNC locally changes the dielectric constant near the GNC surface. Moreover, the absence of broadening or tailing of the plasmon absorption peak indicates that no detectable aggregation occurs during the conjugation.

Bioluminescent Emission Enhancement. As expected, conjugating GNC to nHRP significantly enhances the bioluminescence emission. Figure 2A compares the initial bioluminescence emission rate of BPNs (red columns) and GNC–HRP conjugates (direct conjugates of GNC onto native HRP, black columns). In a series of BPNs (A to D) with increasing GNC/nHRP ratio (average number of GNC on each nHRP), the bioluminescence enhancement factor (luminescence enhancement compared with native HRP as shown by the dashed line) rises from 6.1, 7.0, to 9.5, when the GNC/nHRP ratio increases from (A) 0.5:1, (B) 1:1, to (C) 2:1, respectively. When the GNC/nHRP ratios are higher than (D) 5:1, no further increase in enhancement was observed.

This enhancement can be only achieved when the GNC–HRP distance falls in a narrow suitable range: about 5–20 nm. In a shorter distance (<5 nm),

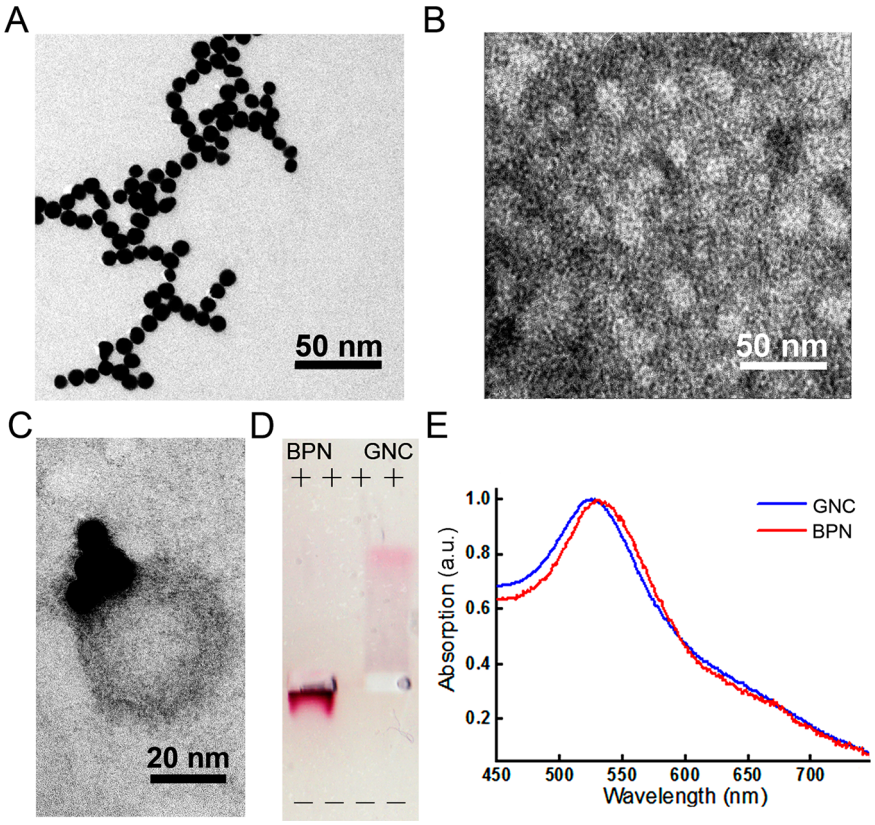

Figure 1. TEM images of (A) gold nanocrystals (GNC), (B) HRP nanocapsules (nHRP), and (C) a bioluminescent protein nanocapsule (BPN). (D) Electrophoresis pattern of GNC and BPN. (E) UV−vis absorption spectra of GNC and BPN.

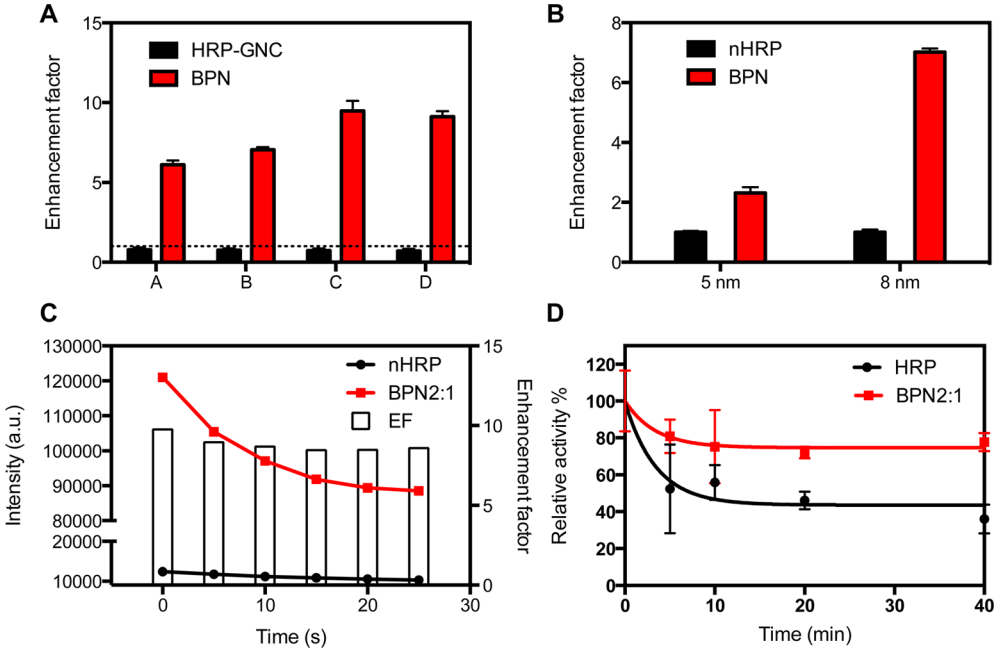

Figure 2. (A) Bioluminescent enhancement factors (normalized to the bioluminescent intensity of native HRP) of BPNs and direct conjugates of GNC and native HRP containing GNC/HRP ratios of (A) 0.5:1, (B) 1:1, (C) 2:1, and (D) 5:1. (B) Bioluminescence enhancement of nHRP−GNC conjugates with different GNC size. (C) Time-dependent bioluminescence intensity of nHRP and BPN2:1. EF (enhancement factor) = intensity(BPN2:1)/intensity(nHRP). (D) Relative residual activity of native HRP and BPNs after incubation at 60 °C.

luminescent emission will be mostly transferred to surface plasmon in a nonradioactive fashion, resulting in bioluminescence quenching; while for a longer distance (>20 nm), no coupling can occur and only

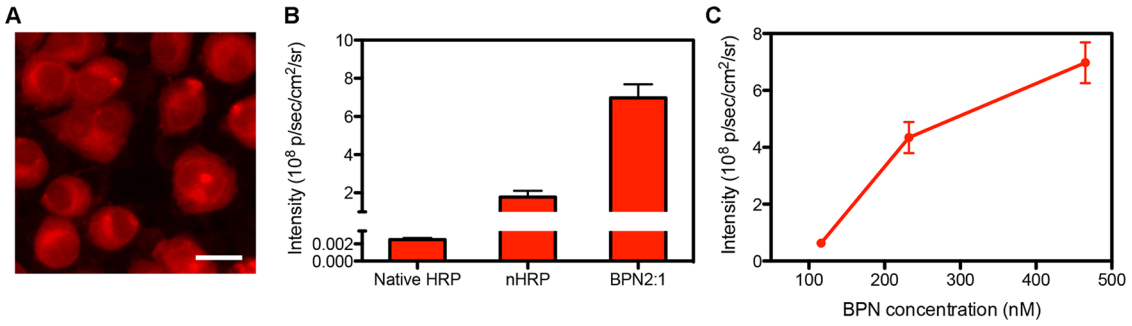

Figure 3. (A) Fluorescent microscope image of HeLa cells treated with BPN2:1 (rhodamine-B-labeled). scale bar = 20 μm. (B) Luminescence intensity of Hela cells treated with native HRP, nHRP, and BPN2:1. (C) Luminescence intensity of Hela cells treated with different concentrations of BPN2:1.

free-space emission will be observed.[4,20] Therefore, optical enhancement requires precise control over the distance between the bioluminescent protein and the metal nanocrystal. In this work, the BPNs are prepared by conjugating GNC onto the nHRP with a thin shell of polymer (~12 nm thick). The polymer shell effectively serves as a spacer between the GNC and the core HRP, assuring a suitable distance for bioluminescence enhancement.

Consistently, owing to the absence of the polymer spacers, the GNC−HRP conjugates synthesized by directly conjugating GNC to the native HRP molecules exhibit significantly lower bioluminescent intensities (Figure 2A, black columns), which are even lower than that generated by native HRP alone (Figure 2A, dashed line). To the best of our knowledge, although metal nanocrystals have been commonly used for fluorescence, chemiluminescence, and phosphorescence enhancement, there is little metal-enhanced bioluminescence reported, probably due to the difficulties in building the required metal−protein spacers. Our design, nevertheless, enables the broad use of near-field optical enhancement for highly sensitive bioluminescence-based analysis.

In addition to the distance between HRP and GNC, the size of the GNC poses a significant influence on the bioluminescence enhancement. Compared with the 8 nm GNC, 5 nm GNC results in much lower bioluminescence intensification (Figure 2B), consistent with the previous observations with metal-enhanced fluorescence and metal-enhanced chemiluminescence.[20,21]

Figure 2C shows the time-dependent bioluminescence intensity of nHRP and BPN2:1. After 25 min incubation, BPN2:1 still retains 8 times higher bioluminescence intensity than nHRP. This study demonstrates that a near 10-fold enhancement of bioluminescent could be achieved using the BPN architecture, confirming our hypothesis of enhancing bioluminescent intensity with noble-metal nanocrystals. Furthermore, BPN exhibits bioluminescence emission with faster decay than that of nHRP. The rate of bioluminescence decay can be fitted in an exponential decay model of $I = C + B\ e^{-kt}$, where I is bioluminescence intensity, C is the intensity at time $t = \infty$, B is a pre-exponential factor, and k is the rate of luminescence depletion with a unit s^{-1}.[22] The rate of depletion of BPN2:1 is 0.12 s^{-1} in comparison with that of nHRP (~0.05 s^{-1}). The 2.4-time faster rate of bioluminescence decay is due to faster depletion of excition-state products.

Enhanced Stability. Besides the dramatically enhanced bioluminescence intensity, and reduced bioluminescence lifetime, this strategy also gifts the encapsulated bioluminescent protein with stability enhancement. As a demonstration, Figure 2D presents the thermal stability of native HRP and BPN, by monitoring HRP residual activity after incubation at elevated temperature. After incubation at 60 °C for 40 min, native HRP lost more than 50% of its original activity. For comparison, BPNs still retained almost 80% of its activity, owning to the well-protected protein conformation by the covalently conjugated polymer shells. In addition, BPNs exhibit excellent stability in biological medium (Supporting Information, Figure S5). After incubation in a cell culture medium, GNC shows a significantly red-shifted visible absorption peak, indicating the aggregation possibly caused by serum proteins. In comparison, the absorption spectrum of BPN does not experience significant changes, indicating the enhanced stability in the biological system of BPN compared with that of GNC. As a summary, increased stabilities preclude the concerns about inactivation during research or clinical applications.

Potential *in Vitro* and *in Vivo* Applications. In addition, BPNs can be effectively delivered into cells without significant toxicity. BPNs display net positive charge on the surface. As demonstrated in our previous work, cells can efficiently internalize cationic nanocapsules *via* endocytosis.[13] Similar cellular internalization was observed with BPNs. Taking the BPNs with a GNC/nHRP ratio of 2:1 (denote as BPN2:1, Column E, Figure 2A) as an example, Figure 3A shows a fluorescence microscope image of Hela cells preincubated with rhodamine-B-labeled BPN2:1 for 2 h at 37 °C. The intense fluorescence signal suggests substantial cell uptake of BPNs. A cell viability assay shows that after 3-h

incubation with different amounts of BPN2:1, Hela cells retain more than 90% of their original viabilities (Supporting Information, Figure S3). Intracellular delivery with low toxicity qualifies our BPN strategy to be applied on intracellularly functional bioluminescent proteins (such as firefly luciferases).

With enhanced bioluminescence, excellent stability, efficient intracellular delivery, and low toxicity, BPN strategy presents itself as a powerful tool for bioluminescence analysis and imaging with both extracellularly and intracellularly functional bioluminescent proteins. As an example, Figure 3B demonstrates the enhanced bioluminescence within the cells by comparing the bioluminescence readout from Hela cells that were preincubated with 465 nM native HRP, nHRP, and BPN2:1. Upon the addition of bioluminescent substrates (luminol and hydrogen peroxide), the bioluminescence produced within the Hela cells was immediately recorded. Native HRP can hardly be delivered into cells, resulting in no observable bioluminescent intensity. nHRP can be efficiently internalized by cells, but with weak bioluminescence. BPN2:1 was effectively delivered into the cells and emitted significantly stronger bioluminescence than nHRP. By further quantifying the bioluminescence enhancement, it was found that, compared with the cells treated with native HRP, HeLa cells treated with BPN2:1 (with the same protein amount) emitted 2000 times higher bioluminescence intensity. Such dramatic bioluminescence enhancement is attributed to significantly improved intracellular delivery and highly effective energy coupling. Note that, when compared with the cells treated with nHRP, the cells treated with BPN2:1 exhibit 4-time enhancement, validating our claim that both intracellular delivery and optical enhancement are critical to achieve optimized performance for intracellular bioluminescence. Additionally, the bioluminescence intensities of the HeLa cells treated with BPN2:1 is concentration-dependent (Figure 3D), allowing fine adjustment of the bioluminescence signal by tuning the dosage. These results predict a great prospect for BPN as an intracellular bioluminescence system.

Bioluminescence enhancement can be also observed *in vivo*. As shown in Supporting Information, Figure S6, we made firefly luciferase-based BPN with a similar protocol. The bioluminescence enhancement is around 2 folds *in vitro* (Figure S6A). Consistently, a similar level of enhancement is observed when the BPN is injected intramuscularly (Figure S6B). These observations indicate that (1) our strategy for bioluminescence enhancement can be applied to various bioluminescence proteins and (2) metal enhanced bioluminescence can be applied to *in vivo* applications.

CONCLUSION

In summary, we have demonstrated a class of bioluminescent protein nanocapsules with significantly enhanced protein stability, intracellular delivery, bioluminescent emission, and rate of bioluminescence depletion. A preliminary *in vivo* study using luciferase-based nanocapsules was also conducted to further demonstrate our hypothesis. As a universal approach, this technique can be extended to construct various bioluminescent nanocapsules for bioluminescence imaging and therapeutic and other applications.

METHODS

Preparation of Gold Nanocrystals. Gold nanocrystals (GNC) were synthesized by citrate reduction followed by surface modification.[23] A 100 mL sample of a 0.01% $HAuCl_4$ solution was heated to boiling under refluxing and stirring in a 250 mL two-neck round-bottom flask, then 3.5 mL of 1% trisodium citrate in water was injected into boiling $HAuCl_4$ solution. The solution was taken away from the heating source after 25 min, and stirring was continued as the solution cooled to room temperature. After that, the GNC concentration was determined by measuring the absorbance of GNC at 506 nm.[2] Then, 15 mL of 0.01 M sodium mercaptopropionate was injected, and the mixture solution was incubated at 50 °C for 8 h. Excess sodium mercaptopropionate was removed by centrifuging and washing.

Encapsulation of HRP. HRP nanocapsules (nHRP) were encapsulated according to the method reported by Du.[15] First, HRP was acryloylated with *N*-acryloxysuccinimide. Then radical polymerization from the surface of the acryloylated HRP was initiated by adding 0.2 mg of ammonium persulfate dissolved in water and 0.4 μL of *N*,*N*,*N*′,*N*′-tetramethylethylenediamine into the test tube. Then a specific amount of *N*-(3-aminopropyl) methacrylamide (APMAAm), acrylamide, and *N*,*N*′-methylene bis(acrylamide) (molar ratio = 3:7:1) dissolved in water was added to the test tube over 60 min. Finally, gel filtration with Sephadex G-75 was used to remove unreacted proteins, monomers, and initiators.

Synthesis of Bioluminescent-Protein Nanocapsules (BPNs). GNC and nHRP was conjugated using ethyl(dimethylaminopropyl) carbodiimide (EDC) and *N*-hydroxysuccinimide (NHS). Briefly, carboxyl groups on as-synthesized GNC was modified with EDC/NHS at 1:10:2(GNC/EDC/NHS) molar ratio and nHRP was mixed together by different molar ratios. Then a specific amount of EDC and NHS (molar ratio = 10:1) was added in the GNC and nHRP solution. The reaction was carried out at room temperature for another 1 h. After that, the conjugates were purified by Sepharose 6B gel filtration columns.

Bioluminescence Measurement. During a measurement, to 975 μL of 20 mM pH 9.0 carbonate buffer, 10 μL of 20 mM luminol (DMSO solution), and 10 μL of 50 mM hydrogenperoxide (aqueous solution) were added. The mixture was vortexed for 15 s, and then 5 μL of HRP or BPN (typically 1 μg/mL) was added and mixed thoroughly. The bioluminescence emission was immediately measured with a Modulus Single Tube Multimode Reader with an integration time of 10 s. For the studies of decay time of the HRP and BPNs, the luminescence was then measured at different time points (every 5 min for 25 min). Relative luminescence intensity is calculated on the basis of the percentage ratio of the emission intensity at a certain time to the intensity at time zero.

BPN Stability Test. For the comparison of thermal stability of HRP and BPN, 0.2 mg/mL native HRP or BPN was incubated in 100 mM pH 7.0 phosphate buffer at 60 °C. At different time intervals, aliquots of HRP or BPN solution were removed and

placed on ice. HRP activity was determined with the chromogenic TMB assay and normalized to the original activity without incubation. To demonstrate the stability of BPNs in biological medium, 60 nM BPN2:1 and 120 nM gold nanocrystal were incubated in phenol red depleted DMEM with a supplement of 10% FBS. After 24 h incubation, the UV−vis spectra of BPN and GNC solutions were recorded with a UV−vis spectrometer.

Cell Bioluminescence Measurement. HeLa cells were cultured in Dulbecco's modified Eagle's medium (DMEM) supplemented with 10% bovine growth serum (BGS) and 1% penicillin/streptomycin. Cells (10 000 cells/well, 96-well plate) were seeded the day before adding HRP, nHRP, or BPN2:1. HRP, nHRP, or BPN2:1 with different concentrations (116 nM, 232 nM, and 465 nM) were added into the cell medium. After incubation at 37 °C for 3 h, the cells were washed three times with PBS. After that, 100 μL of PBS containing 200 nM luminol and 500 nM hydrogenperoxide were added to each well. The bioluminescence image of the cells was immediately captured by a cooled charge coupled device (CCD) camera (IVIS, Xenogen) with an exposure time of 1 min.

Conflict of Interest: The authors declare no competing financial interest.

Acknowledgment. This research was financially supported by the Defense Threat Reducing Agency (DTRA) and International Science & Technology Cooperation Program of China (2012DFA51690). We would like to thank Cynthia Cam for her help with the animal studies.

Supporting Information Available: Full experimental details for preparation of bioluminescent-protein nanocapsules; particle size of HRP nanocapsules; zeta potential of bioluminescent-protein nanocapsules; cell viability results; cell internalization protocols. This material is available free of charge *via* the Internet at http://pubs.acs.org.

REFERENCES AND NOTES

1. Miyawaki, A. Bringing Bioluminescence into the Picture. *Nat. Methods* **2007**, *4*, 616–617.
2. Dragulescu-Andrasi, A.; Chan, C. T.; De, A.; Massoud, T. F.; Gambhir, S. S. Bioluminescence Resonance Energy Transfer (BRET) Imaging of Protein−Protein Interactions within Deep Tissues of Living Subjects. *Proc. Natl. Acad. Sci. U.S.A.* **2011**, *108*, 12060–12065.
3. Badr, C. E.; Tannous, B. A. Bioluminescence Imaging: Progress and Applications. *Trends Biotechnol.* **2011**, *29*, 624–633.
4. Aslan, K.; Geddes, C. D. Metal-Enhanced Chemiluminescence: Advanced Chemiluminescence Concepts for the 21st Century. *Chem. Soc. Rev.* **2009**, *38*, 2556–2564.
5. Karolin, J. O.; Geddes, C. D. Reduced Lifetimes Are Directly Correlated with Excitation Irradiance in Metal-Enhanced Fluorescence (MEF). *J. Fluoresc.* **2012**, *22*, 1659–1662.
6. Aslan, K.; Malyn, S. N.; Geddes, C. D. Metal-Enhanced Fluorescence from Gold Surfaces: Angular Dependent Emission. *J. Fluoresc.* **2007**, *17*, 7–13.
7. Aslan, K.; Wu, M.; Lakowicz, J. R.; Geddes, C. D. Fluorescent Core−Shell Ag@SiO_2 Nanocomposites for Metal-Enhanced Fluorescence and Single Nanoparticle Sensing Platforms. *J. Am. Chem. Soc.* **2007**, *129*, 1524–1525.
8. Zhang, Y.; Mandeng, L. N.; Bondre, N.; Dragan, A.; Geddes, C. D. Metal-Enhanced Fluorescence From Silver−SiO_2−Silver Nanoburger Structures. *Langmuir* **2010**, *26*, 12371–12376.
9. Chowdhury, M. H.; Aslan, K.; Malyn, S. N.; Lakowicz, J. R.; Geddes, C. D. Metal-Enhanced Chemiluminescence: Radiating Plasmons Generated From Chemically Induced Electronic Excited States. *Appl. Phys. Lett.* **2006**, *88*, 173104.
10. Chowdhury, M. H.; Aslan, K.; Malyn, S. N.; Lakowicz, J. R.; Geddes, C. D. Metal-Enhanced Chemiluminescence. *J. Fluoresc.* **2006**, *16*, 295–299.
11. Zhang, Y.; Aslan, K.; Previte, M. J. R.; Malyn, S. N.; Geddes, C. D. Metal-Enhanced Phosphorescence: Interpretation in Terms of Triplet-Coupled Radiating Plasmons. *J. Phys. Chem. B* **2006**, *110*, 25108–25114.
12. Kim, Y.-P.; Daniel, W. L.; Xia, Z.; Xie, H.; Mirkin, C. A.; Rao, J. Bioluminescent Nanosensors for Protease Detection Based upon Gold Nanoparticle−Luciferase Conjugates. *Chem. Commun. (Cambridge)* **2010**, *46*, 76.
13. Yan, M.; Du, J.; Gu, Z.; Liang, M.; Hu, Y.; Zhang, W.; Priceman, S.; Wu, L.; Zhou, Z. H.; Liu, Z.; et al. A Novel Intracellular Protein Delivery Platform Based on Single-Protein Nanocapsules. *Nat. Nanotechnol.* **2010**, *5*, 48–53.
14. Gu, Z.; Yan, M.; Hu, B.; Joo, K.-I.; Biswas, A.; Huang, Y.; Lu, Y.; Wang, P.; Tang, Y. Protein Nanocapsule Weaved with Enzymatically Degradable Polymeric Network. *Nano Lett.* **2009**, *9*, 4533–4538.
15. Du, J.; Yu, C.; Pan, D.; Li, J.; Chen, W.; Yan, M.; Segura, T.; Lu, Y. Quantum-Dot-Decorated Robust Transductable Bioluminescent Nanocapsules. *J. Am. Chem. Soc.* **2010**, *132*, 12780–12781.
16. Biswas, A.; Joo, K.-I.; Liu, J.; Zhao, M.; Fan, G.; Wang, P.; Gu, Z.; Tang, Y. Endoprotease-Mediated Intracellular Protein Delivery Using Nanocapsules. *ACS Nano* **2011**, *5*, 1385–1394.
17. Yan, M.; Ge, J.; Liu, Z.; Ouyang, P. Encapsulation of Single Enzyme in Nanogel with Enhanced Biocatalytic Activity and Stability. *J. Am. Chem. Soc.* **2006**, *128*, 11008–11009.
18. Ge, J.; Lu, D.; Wang, J.; Yan, M.; Lu, Y.; Liu, Z. Molecular Fundamentals of Enzyme Nanogels. *J. Phys. Chem. B* **2008**, *112*, 14319–14324.
19. Henriksen, A.; Schuller, D. J.; Meno, K.; Welinder, K. G.; Smith, A. T.; Gajhede, M. Structural Interactions between Horseradish Peroxidase C and the Substrate Benzhydroxamic Acid Determined by X-ray Crystallography. *Biochemistry* **1998**, *37*, 8054–8060.
20. Chen, J.; Jin, Y.; Fahruddin, N.; Zhao, J. X. Development of Gold Nanoparticle-Enhanced Fluorescent Nanocomposites. *Langmuir* **2013**, *29*, 1584–1591.
21. Duan, C.; Cui, H.; Zhang, Z.; Liu, B.; Guo, J.; Wang, W. Size-Dependent Inhibition and Enhancement by Gold Nanoparticles of Luminol-Ferricyanide Chemiluminescence. *J. Phys. Chem. C* **2007**, *111*, 4561–4566.
22. Chowdhury, M. H.; Malyn, S. N.; Aslan, K.; Lakowicz, J. R.; Geddes, C. D. Multicolor Directional Surface Plasmon-Coupled Chemiluminescence. *J. Phys. Chem. B* **2006**, *110*, 22644–22651.
23. Zhu, T.; Vasilev, K.; Kreiter, M.; Mittler, S.; Knoll, W. Surface Modification of Citrate-Reduced Colloidal Gold Nanoparticles with 2-Mercaptosuccinic Acid. *Langmuir* **2003**, *19*, 9518–9525.